

An optimized process for fabrication of SrBi₂Ta₂O₉ thin films using a novel chemical solution deposition technique

Seung-Hyun Kim, D.J. Kim, K.M. Lee, M. Park, and A.I. Kingon
*Department of Materials Science and Engineering, North Carolina State University,
Raleigh, North Carolina 27695*

R.J. Nemanich
Department of Physics, North Carolina State University, Raleigh, North Carolina 27695

J. Im and S.K. Streiffer
Materials Science Division, Argonne National Laboratory, Argonne, Illinois 60439

(Received 30 October 1998; accepted 18 August 1999)

Ferroelectric SrBi₂Ta₂O₉ (SBT) thin films on Pt/ZrO₂/SiO₂/Si were successfully prepared by using an alkanolamine-modified chemical solution deposition method. It was observed that alkanolamine provided stability to the SBT solution by retarding the hydrolysis and condensation rates. The crystallinity and the microstructure of the SBT thin films improved with increasing annealing temperature and were strongly correlated with the ferroelectric properties of the SBT thin films. The films annealed at 800 °C exhibited low leakage current density, low voltage saturation, high remanent polarization, and good fatigue characteristics at least up to 10¹⁰ switching cycles, indicating favorable behavior for memory applications.

I. INTRODUCTION

In recent years, ferroelectric thin films have been extensively investigated for nonvolatile memory applications.¹⁻³ Although Pb(Zr_xTi_{1-x})O₃ (PZT) materials have been considered to be promising candidates for these applications,⁴⁻⁶ PZT thin films undergo severe polarization fatigue with metal electrodes,^{6,7} which may limit their applicability. Recently, it has been reported that Sr Bi₂Ta₂O₉ (SBT) layer-structured ferroelectric thin films have high potentials for memory applications due to good fatigue resistance and low voltage polarization switching.^{8,9}

Among various preparation techniques for SBT thin films, chemical solution deposition (CSD) is promising because it provides high purity, large deposition area, and easy composition control.^{10,11} However, a stable, simple preparation process for SBT solutions has not previously been reported due to limitations of preferred precursors.

In this study, a new chemical route using an alkanolamine as a chelating agent is suggested. It is found that a particular chelating agent increases the stability of the SBT solution. The optimal processing window for producing SBT thin films using this new chemical solution method is reported here. We also make a comparative investigation of surface microstructures, crystallization behaviors, and related ferroelectric properties for SBT thin films prepared using this method as a function of annealing temperature.

II. EXPERIMENTAL

The choice of precursors, solvents and chelating agents is very important for producing high-quality thin films using chemical solution deposition (CSD) processing. In this work, SBT solution (Sr/Bi/Ta = 0.8/2.3/2) was prepared using Sr-acetate [Sr(CH₃CO₂)₂], Bi-nitrate [Bi(NO₃)₃ · 5H₂O], and Ta-ethoxide [Ta(OC₂H₅)₅] as precursors. Acetic acid for Bi and methanol for Sr and Ta were used as solvents. In the CSD method, hydrolysis and condensation rates are an important factor that must be controlled to maximize solution stability. In general, in order to reduce the reactivity of hydrolysis and condensation, complexing or chelating agents are needed.^{12,13} In this study, we used alkanolamine as a complexing agent for the SBT solution. Alkanolamine is an alkoxy alcohol used for formation of homogeneous products and to enhance stability of the gel, by reducing the hydrolysis reaction rate.^{2,14}

Films were spin coated onto Pt/ZrO₂/SiO₂/Si substrate at 3000 rpm for 30 s and subsequently dried at 260 °C for 5 min, 450 °C for 10 min, and 700 °C for 3 min for each layer. The coated films were annealed at 700, 750, or 800 °C for 1 h in O₂ through direct insertion into a tube furnace. Final film thickness was 200 nm by scanning electron microscopy (SEM). For electrical measurements, Pt top electrodes (area = 3.96 × 10⁻⁴ cm²) were deposited on the SBT thin films by ion-beam sputter deposition. Crystallization behavior and film orientation were investigated using an x-ray diffractometer operated

Cu K_α radiation; polarization–electric (P-E) field hysteresis loops and fatigue properties of the films were investigated using a Radiant RT66A ferroelectric tester.

III. RESULTS AND DISCUSSION

In general, metal alkoxides have a tendency to react easily with H₂O containing OH⁻¹ ligands due to their low electronegativity, high partial charge, and the large ionic radius of metal ions.^{14,15} To maximize solution stability, hydrolysis and condensation rates must be controlled. In this study, we used alkanolamine as a complexing agent for the SBT solution, so as to reduce the reactivity of the hydrolysis and condensation. In addition to its complexing effects, alkanolamine has excellent dissolving power for Sr acetate. However, in the case of SBT solutions, the Bi precursor has a serious limitation for solubility with an alcohol or alkanolamine. It is soluble only with acetic acid, and this makes it difficult to easily prepare stable solutions.

In the preparation of the SBT solution, acetic acid serves as more than a simple solvent; it might act as a chemical modifying agent by reacting with the alkoxide precursors at a molecular level, replacing at least some of the alkoxy groups, and thus, altering the hydrolysis and condensation characteristics of the precursors. However, in this case, acetic acid can also lead to the production of reaction by-products such as free alcohols and the formation of water and ester compounds such as methyl or ethyl acetate. Figure 1 displays Fourier transform infrared (FTIR) spectra of an SBT solution as a function of aging time, in order to investigate stability and structure of the solution. The predominant spectral features include two intense bands centered at ~1570 and ~1440 cm⁻¹, which are due to the asymmetric and symmetric COO stretching vibrations of the acetate ligand, respectively. The band separation of ~130 cm⁻¹ shows bidentate acetate coordination; however, it is not possible to determine whether acetate groups are bridging or simply chelating from these peaks. The simple implication of the fact that one of these peaks is present as a multiple, and that the other peak shows a distinct shoulder, might be indicative of bridging acetate groups of different nature and that these bands confirm that acetic acid reacts with the alkoxide precursors at a molecular level.

The presence of other bands in the FTIR spectra is also very important. The shoulder at ~1250 cm⁻¹ and the peak at 1740 cm⁻¹ are consistent with the formation of an ester compound. This by-product is possibly formed due to the reaction of acetic acid with an alcohol. This reaction can lead to the formation of water, which may continuously induce the hydrolysis and condensation of the precursors, leading to degradation of the solution with increased aging time. To compensate for these drawbacks, we used alkanolamine to reduce the hydrolysis and condensation

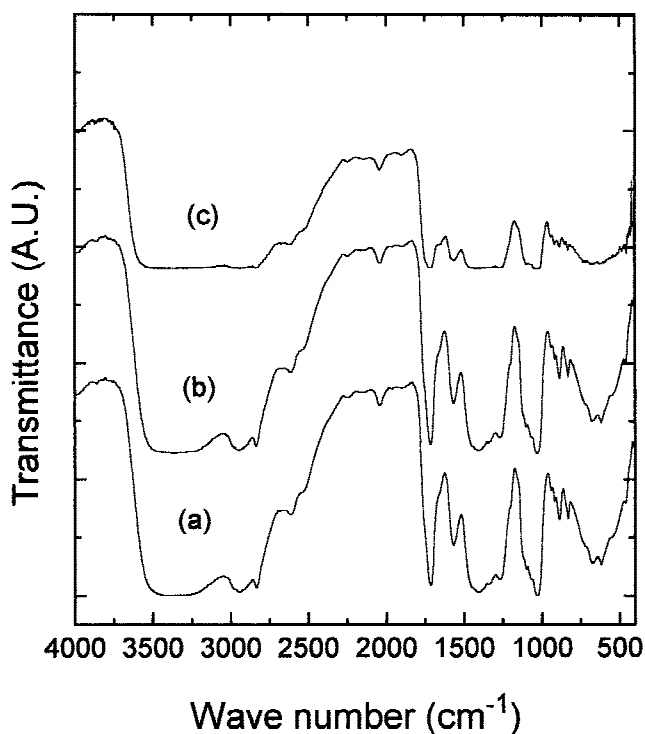


FIG. 1. FTIR spectra of an SBT solution as a function of aging time: (a) 1 day, (b) 1 month, and (c) 3 months.

reaction. Alkanolamine as a complexing agent causes steric hindrance and inductive effects, which reduce the reaction of water with alkoxide precursor and improve stability of the solution with aging time.^{2,14} As shown in Figs. 1(a) and 1(b), the FTIR spectra of the solution are not significantly changed up to 1 month. This implies that the solution is quite stable in this period without any change of solution properties.

However, FTIR spectra of a solution aged 3 months show significant changes as compared to Figs. 1(a) and 1(b). It is found that most of the peaks of the FTIR spectra are suppressed, particularly peaks below 1000 cm⁻¹ related to metal–oxygen (M–O), implying the loss of solution properties. As a result, we can expect that the optimal processing window for stability of the alkanolamine-modified SBT solution is at least up to 1 month.

Figure 2 shows differential thermal analysis (DTA) and thermogravimetric analysis (TGA) curves of SBT gel powder in the range from room temperature to 800 °C. The DTA curve shows endothermic behavior below 200 °C due to desorption of absorbed H₂O and evaporation of the solvents with low boiling points such as methanol and free alcohol. The exothermic peaks below 400 °C correspond to removal and decomposition of nonreacted alkanolamine, and by-products of organic compounds formed by hydrolysis and condensation reactions. The broad peaks at high temperature might be mainly attributed to crystallization of the SBT gel pow-

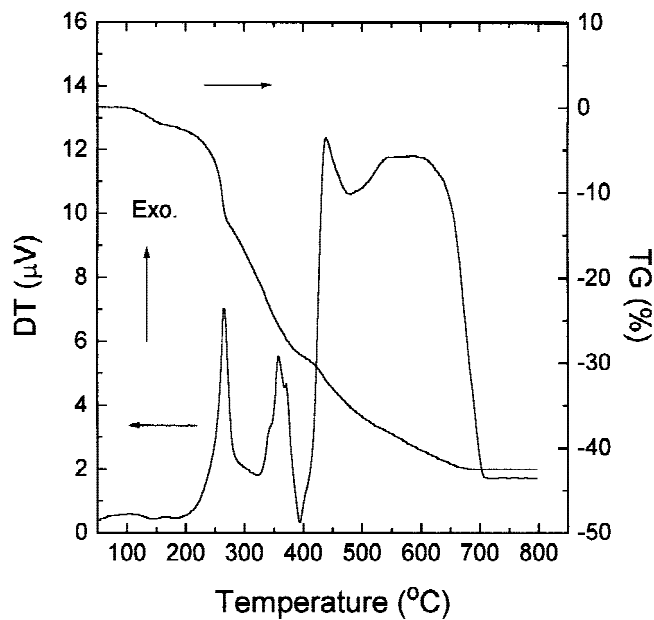


FIG. 2. DTA and TGA curves of SBT gel powder.

der. However, because a large weight loss is observed in the TGA curve in this temperature range, the peaks seem to be overlapped with the peaks arising from the decomposition of residual organics and bridged or reacted alkanolamine. The TGA curve shows about 40% weight loss in total due to evaporation of the solvents and decomposition of organic groups.

The drying condition for the decomposition of residual organics in the films is determined on the basis of thermal analysis of the SBT gel powder, even if the decomposition temperature of residual organics for the film and the powder is not identical. Successful preparation of SBT thin films requires that the films should be free from cracks and processing-induced defects. In general, large internal stress causes cracking due to the volume change during the drying and firing process of a wet-coated film.^{16,17} This internal stress can be partially relaxed by controlling the drying process, that is, by carefully selecting the drying temperature steps. For this reason, the drying process accompanied by the pyrolysis of organometallic compounds is a critical step in film preparation. Drying steps also establish the precrystallization conditions, including perhaps at least to some degree the metal coordination, that may be necessary to crystallize a well-ordered film. On the basis of the temperature where the main solvent and residual organics are removed, the drying of the SBT thin films is carried out in three steps at 260, 450, and 700 °C.

Figure 3 shows x-ray diffraction (XRD) patterns as a function of film-annealing temperature, carried out at 700, 750, and 800 °C in an oxygen atmosphere for 1 h. It is possible to obtain a pure perovskite phase at the an-

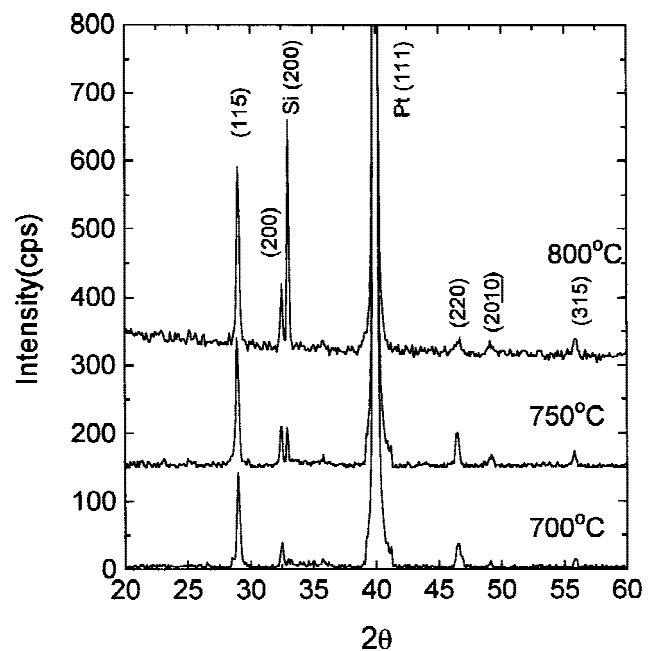


FIG. 3. XRD patterns of SBT thin films as a function of annealing temperature.

nealing temperature of 700 °C. However, longer annealing time and higher annealing temperature are required for SBT thin films to become well crystallized with respect to PZT thin films.² The peak intensity and sharpness in the XRD patterns are found to increase with increasing annealing temperature, indicating better crystallinity and surface microstructure of the films. The XRD patterns reveal that the films are polycrystalline in nature with highly textured (115) orientation.

SEM images of SBT thin films annealed at 700, 750, and 800 °C in O₂ for 1 h are shown in Figs. 4(a), 4(b), and 4(c), respectively. It is observed that density and uniformity of the films increase with increasing annealing temperature, indicating improvements in microstructure. The SBT film annealed at 700 °C in Fig. 4(a) shows a porous and locally inhomogeneous microstructure. In contrast, the surface morphologies of the films annealed at 750 and 800 °C as shown in Figs. 4(b) and 4(c) show well-developed grain structure. These two films show very similar surface features with uniformly distributed grain islands. Increasing annealing temperature from 700 to 800 °C does not lead to any obvious increase of grain size. Frequently, SBT thin films produced by other methods have asymmetric, wormlike morphologies;^{18,19} however, alkanolamine-modified films show spherical grain and dense structure. The average grain size of the films is approximately 0.2–0.3 μm.

Figure 5 shows polarization–voltage (P-V) hysteresis loops of SBT thin films as a function of annealing temperature, measured from 1 to 5 V. It is observed that the

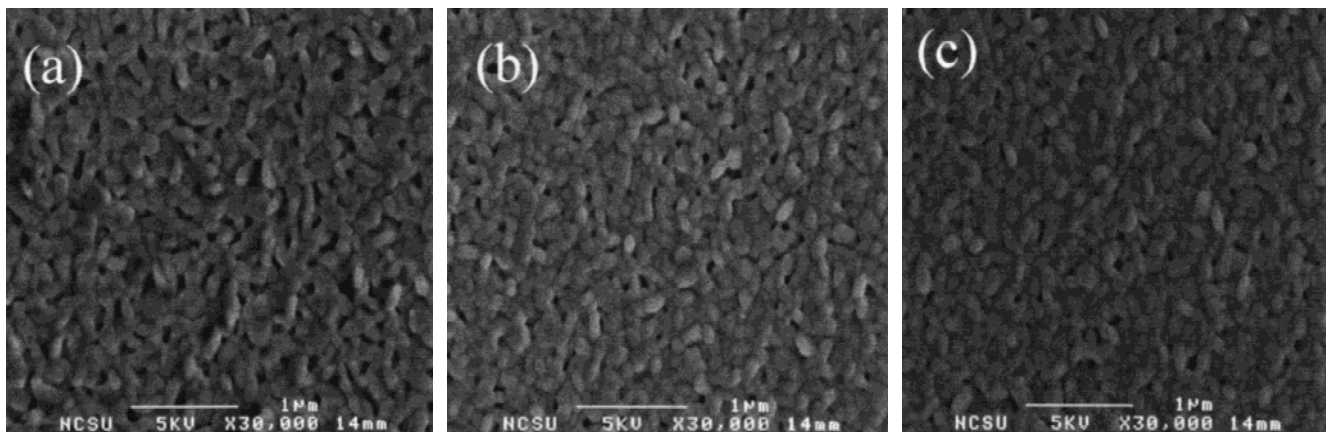


FIG. 4. SEM micrographs of SBT thin films annealed at (a) 700 °C, (b) 750 °C, and (c) 800 °C in O₂ for 1 h.

values of remanent polarization (P_r) and coercive voltage (V_c) increase and the P-V hysteresis loops reveal well-saturated shapes with increasing annealing temperatures and applied voltages. The typical hysteresis loop of the SBT thin film annealed at 800 °C is obtained at 2 V, and it is fully saturated even below an applied voltage of 3 V ($2P_r \approx 16 \mu\text{C}/\text{cm}^2$). The measured $2P_r$ value of the SBT thin film at 5 V is almost $20 \mu\text{C}/\text{cm}^2$. The SBT film annealed at 750 °C reveals a somewhat smaller P_r value ($2P_r \approx 15 \mu\text{C}/\text{cm}^2$ at 5 V) as compared to the film annealed at 800 °C, but shows a very similar trend as a function of applied voltage. However, the film annealed at 700 °C has a very low P_r value ($2P_r \approx 7 \mu\text{C}/\text{cm}^2$ at 5 V), and it is not saturated even at high applied voltage of 5 V, even though the XRD pattern indicates the perovskite phase with little detectable secondary phase. We can postulate that there is some type of unoriented, nanocrystalline second phase or locally inhomogeneous crystallization behavior of the film. If this is the case, either no diffraction peaks or peaks of only very low intensity would be present even though a pure perovskite phase of the films is detected by XRD.

To further investigate the structure and the crystallization behavior of the SBT thin films, micro-Raman spectroscopy was performed with the 514.5-nm line of an Ar ion laser. Because the diameter of the focused laser beam is $\sim 5 \mu\text{m}$, it is possible to analyze a very localized area of each sample. Raman spectra were collected from two different regions (center and edge) of the films, to determine if the films are formed by a spatially homogeneous crystallization process.

The irreducible representation for tetragonal SBT films with $I4/mmm$ symmetry can be expressed as²⁰

$$\Gamma = 4A_{1g} + 2B_{1g} + 6E_g + 7A_{2u} + B_{2u} + 8E_u \quad (1)$$

Among these modes, $4A_{1g}$, $2B_{1g}$, and $6E_g$ modes are Raman active. For orthorhombic SBT, the degeneracy of the E_g mode is lifted by splitting it into B_{2g} and B_{3g} .

Figure 6 shows the Raman spectra from SBT thin films as a function of annealing temperature. The position and the full-width at half maximum (FWHM) of the Raman peaks as indicated on the figure are determined by fitting with Voigt functions. Three peaks are observed from the substrate (Pt/ZrO₂/SiO₂/Si). These are detected at ~ 116 , ~ 160 , and $\sim 268 \text{ cm}^{-1}$. The SBT Raman band at $\sim 207 \text{ cm}^{-1}$ is assigned to the O-Ta-O bending mode ($B_{2g} + B_{3g}$).²¹ The band at $\sim 599 \text{ cm}^{-1}$ is associated with a Ta-O-Ta mode. These bands, which share their oxygen atom with another Ta atom, are similar to those found in perovskite niobates. The peak at 810 cm^{-1} is produced by the A_{1g} mode due to the stretching of TaO₆ octahedra.²²

As can be seen from Fig. 6, the FWHM of the peaks at 599 and 810 cm^{-1} decreases with increasing the annealing temperature from 700 to 800 °C. The Raman spectra indicate that the films annealed at 750 and 800 °C are relatively well crystallized, and the crystallinity of the films is relatively homogeneous across the sample. The film annealed at 700 °C, however, shows inhomogeneity in crystallinity, because the center and edge of the film yield different Raman spectra. The spectrum of the center of the film does not show any Raman peaks except those of the substrates. It implies that the center of the film has poor crystallinity as compared to the edge of the film. As a result of XRD, SEM, and Raman analysis, the crystallinity and the uniformity of the SBT thin films are found to improve with increasing annealing temperature, and this in turn is strongly correlated with the ferroelectric properties of the SBT thin films.

Another important factor for ferroelectric properties of SBT thin films such as polarization is film orientation.²³ To clarify the impact of orientation on the polarization behavior of these films, we fabricated a film with a mixed (00l)/(115) orientation by changing the drying condition and substrate treatment, instead of the highly textured (115) orientation. We will discuss the control of the film orientation in another paper in detail. Figure 7

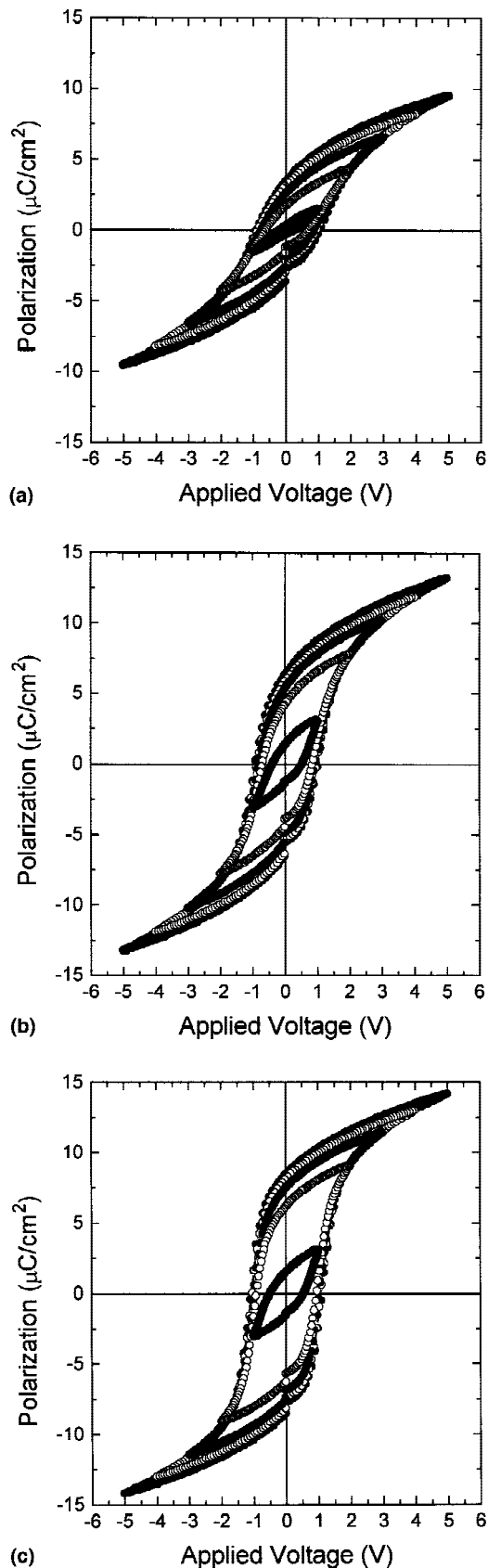


FIG. 5. P-V hysteresis loops of SBT thin films annealed at (a) 700 °C, (b) 750 °C, and (c) 800 °C in O₂ for 1 h.

and Fig. 8 show the XRD pattern and the P-V hysteresis loops, respectively, of this film annealed at 800 °C in oxygen atmosphere for 1 h. It is observed that (00 l) oriented film has a much lower P_r as compared to that of (115) oriented film. The $2P_r$ value of this film measured with an applied voltage of 5 V is just 9 $\mu\text{m}/\text{cm}^2$. This is consistent with previous observation of no or little spontaneous polarization along the c axis in SBT.^{8,24}

Leakage current density is another important consideration for device application. In general, SBT-based capacitors show low leakage current density at low applied voltage (<5 V) even for small film thicknesses (<100 nm).^{9,25} Figure 9 shows the leakage current density of these SBT thin films as a function of annealing temperature and applied voltage. The leakage current density of the films is decreased with increasing annealing temperature. This is consistent with the conclusions drawn from microstructural characterization above, that the microstructure of the film annealed at high temperature shows a dense and well-developed grain structure with good crystallinity, whereas the more porous microstructure of the 700 °C annealed sample can provide easy leakage paths. The leakage current density of the film annealed at 800 °C is around 10^{-7} A/cm² up to 8 V; however, the leakage current density increases abruptly above 8 V.

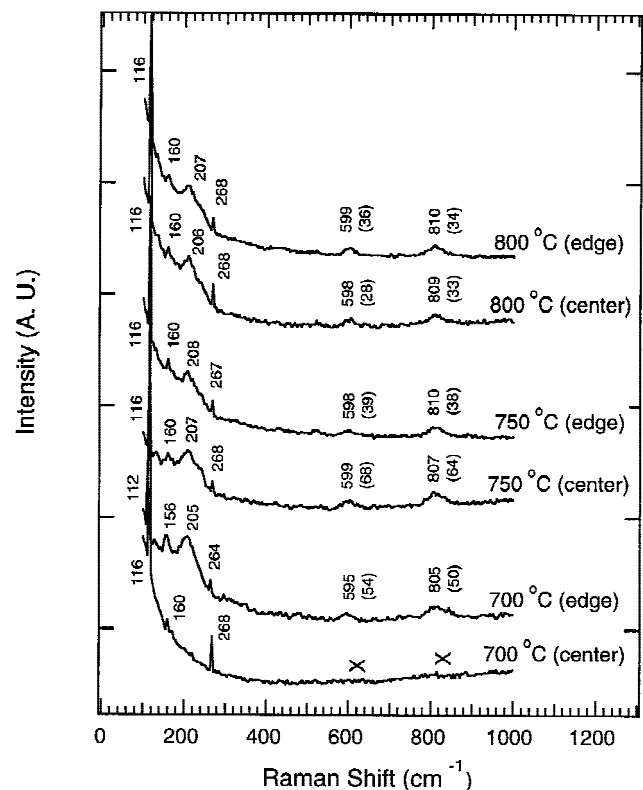


FIG. 6. Raman spectra of SBT thin films as a function of annealing temperature. Peak position and FWHM (in parentheses) are indicated for selected peaks.

Figure 10 shows fatigue properties of SBT thin films measured at 500 kHz, and 5 V. All the films exhibit negligible polarization fatigue even with Pt electrode up to 10¹⁰ cycles. These fatigue results confirm that the films produced using the techniques described here are of high quality.

IV. CONCLUSIONS

A new chemical route for deposition of SBT films is demonstrated, which uses an alkanolamine as a chelating agent for SBT the solution. The alkanolamine-stabilized solution has a lifetime of at least 1 month without any

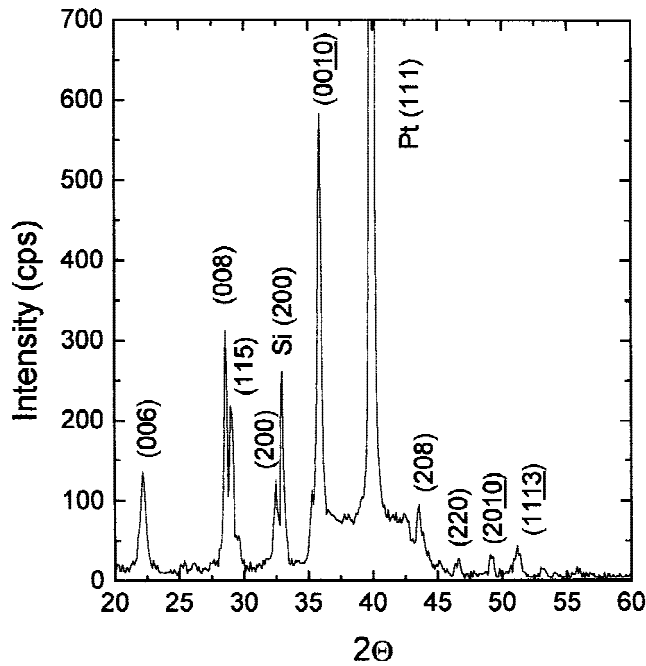


FIG. 7. XRD pattern of SBT thin film with a mixed (115)/(00) orientation.

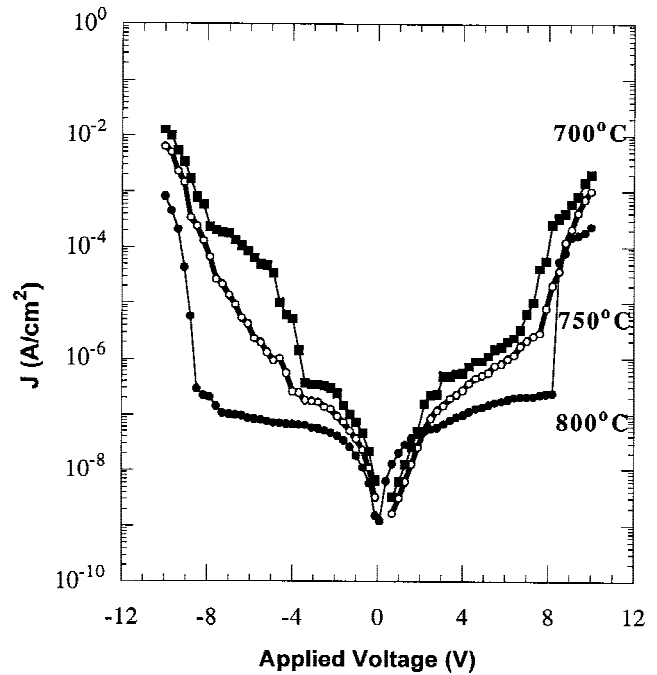


FIG. 9. Current density–voltage curves of SBT thin films as a function of annealing temperature.

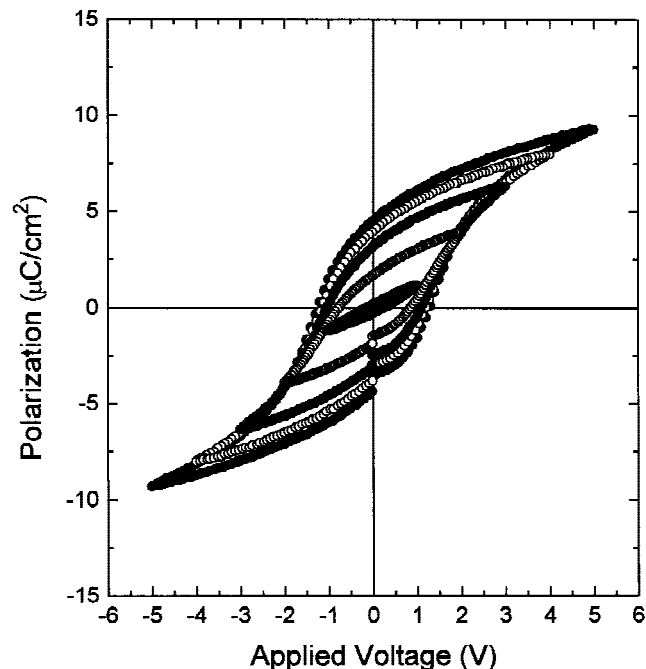


FIG. 8. P-V hysteresis loops of SBT thin film with a mixed (115)/(00) orientation.

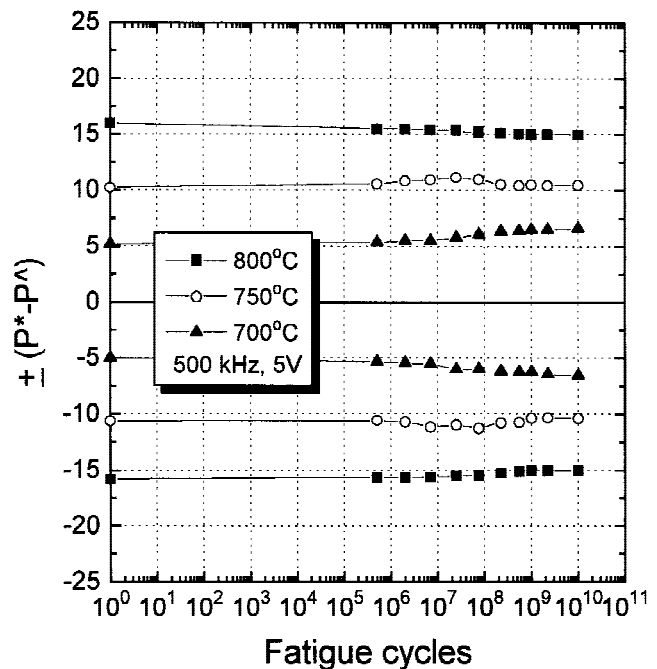


FIG. 10. Fatigue behaviors of SBT thin films as a function of annealing temperature, measured at 500 kHz and 5 V.

appreciable change of the solution properties. The films fabricated from this solution and annealed at a temperature of 800 °C exhibit low leakage current density, low voltage saturation, and high remanent polarization as compared to those of low-temperature annealed films. XRD, SEM, and Raman spectroscopy indicate that the improvement in properties with higher annealing temperature is due to improved film density and crystal quality, as indicated by sharpening of the Raman peaks for the SBT vibrational modes. These SBT thin films exhibit negligible polarization fatigue even with Pt electrodes up to at least 10¹⁰ cycles, indicating favorable behavior for memory applications.

ACKNOWLEDGMENTS

This work was supported by Ramtron International Corporation, and by a gift from LG Semicon. We are thankful for useful discussions with other members of the Kingon research group.

REFERENCES

1. K.K. Deb, K.W. Bennett, P.S. Brody, and B.M. Melnick, *Integrated Ferroelectrics* **6**, 253 (1995).
2. S-H. Kim, D-J. Kim, S.K. Streiffer, and A.I. Kingon, *J. Mater. Res.* **14**, 2476 (1999).
3. H.N. Al-Shareef, O. Auciello, and A.I. Kingon, *J. Appl. Phys.* **77**, 2146 (1995).
4. I.S. Chung, J.K. Lee, W.I. Lee, C.W. Chung, and S.B. Desu, in *Ferroelectric Thin Films*, edited by B.A. Tuttle, S.B. Desu, R. Ramesh, and T. Shiosaki (Mater. Res. Soc. Symp. Proc. **361**, Pittsburgh, PA, 1995), p. 249.
5. J. Chen, K.R. Udayakumar, K.G. Brooks, and L.E. Cross, *J. Appl. Phys.* **71**, 4465 (1992).
6. S-H. Kim, J.G. Hong, S.K. Streiffer, and A.I. Kingon, *J. Mater. Res.* **14**, 1018 (1999).
7. T. Mihara, H. Watanabe, and C.A. Paz de Araujo, *Jpn. J. Appl. Phys.* **33**, 528 (1994).
8. K. Amanuma, T. Hase, and Y. Miyasaka, *Appl. Phys. Lett.* **66**, 222 (1995).
9. C.A. Paz de Araujo, J.D. Cuchiaro, L.D. Mcmillan, M.C. Scott, and J.F. Scott, *Nature* **374**, 627 (1995).
10. P.C. Joshi, S.O. Ryu, S. Tirumala, and S.B. Desu, in *Ferroelectric Thin Films*, edited by R.E. Treece, R.E. Jones, C.M. Foster, S.B. Desu, and I.K. Yoo (Mater. Res. Soc. Symp. Proc. **493**, Warrendale, PA, 1998), p. 215.
11. S-H. Kim, C.E. Kim, and Y.J. Oh, *Thin Solid Films* **305**, 321 (1997).
12. R.W. Schwartz, T.J. Boyle, S.J. Lockwood, M.B. Sinclair, D. Dimos, and C.D. Buchheit, *Integrated Ferroelectrics* **7**, 259 (1995).
13. G. Yi, Z. Wu, and M. Sayer, *J. Appl. Phys.* **64**, 2717 (1988).
14. S-H. Kim, C.E. Kim, and Y.J. Oh, *J. Mater. Sci.* **30**, 5639 (1995).
15. C. Sanchez, J. Livage, M. Henry, and F. Babonneau, *J. Non-Cryst. Solids* **100**, 65 (1988).
16. G. Yi and M. Sayer, *Ceram. Bull.* **70**, 1175 (1991).
17. G.W. Scherer, *J. Am. Ceram. Soc.* **73**, 3 (1990).
18. Y. Ito, M. Ushikubo, S. Yokoyama, T. Atsuki, T. Yonezawa, and K. Ogi, *Integrated Ferroelectrics* **14**, 123 (1997).
19. T.J. Boyle, C.D. Buchheit, M.A. Rodriguez, H.N. Al-Shareef, B. Scott, and J.W. Ziller, *J. Mater. Res.* **11**, 1 (1996).
20. M.P. Moret, R. Zallen, R.E. Newnham, P.C. Joshi, and S.B. Desu, *Phys. Rev. B* **57**, 5715 (1998).
21. W. Perez, E. Ching-Prado, A. Reynes-Figueroa, R.S. Katiyar, D. Ravichandran, and A.S. Bhalla, in *Ferroelectric Thin Films*, edited by R.E. Treece, R.E. Jones, C.M. Foster, S.B. Desu, and I.K. Yoo (Mater. Res. Soc. Symp. Proc. **493**, Warrendale, PA, 1998), p. 237.
22. E. Husson, L. Abello, and A. Morell, *Mater. Res. Bull.* **25**, 539 (1990).
23. M. Nagata, D.P. Vijay, X. Zhang, and S.B. Desu, *Phys. Status Solidi A* **157**, 75 (1996).
24. X. Du and I. Chen, in *Ferroelectric Thin Films*, edited by R.E. Treece, R.E. Jones, C.M. Foster, S.B. Desu, and I.K. Yoo (Mater. Res. Soc. Symp. Proc. **493**, Warrendale, PA, 1998), p. 261.
25. K. Amanuma and T. Kunio, *Integrated Ferroelectrics* **16**, 175 (1997).